Journal of Alloys and Compounds 509S (2011) S801–S803

Contents lists available at ScienceDirect

Journal of Alloys and Compounds

journal homepage: www.elsevier.com/locate/jallcom

Hydrogen trapping properties of Zr-based intermetallic compounds in the presence of CO contaminant gas

Jocelyn Prigent[a], Michel Latroche[a,*], Elisa Leoni[b], Valentin Rohr[b]

[a] Chimie Métallurgie des Terres Rares, ICMPE-UMR 7182, CNRS, 2-8 rue Henri Dunant, 94320 Thiais, France
[b] AREVA NC, 1, rue des Hérons, 78182 Montigny Le Bretonneux, France

ARTICLE INFO

Article history:
Received 13 August 2010
Received in revised form 27 October 2010
Accepted 28 October 2010
Available online 10 November 2010

Keywords:
Hydrogen absorbing materials
Intermetallics
Powder metallurgy
Kinetics

ABSTRACT

Intermetallic compounds, as hydrogen getters, are considered to control the quantity of hydrogen generated in radioactive waste packaging. The compounds ZrCo, Zr_2Fe and a Zr-rich Zr–Ti–V alloy have been chosen as they form very stable hydrides at ambient temperature. However, other gases are produced in the packaging such as carbon monoxide, a gas known to poison the surface of intermetallic compounds and to hinder the hydrogen sorption reaction. The three Zr-based compounds have been first characterized regarding their metallurgical state and their gas sorption properties toward pure hydrogen. Then, the sorption properties of the activated materials have been studied using a mixture of 5 vol.% CO + 95 vol.% H_2. We demonstrated that though the presence of CO sharply slows down the reaction rate the activated compounds still show significant sorption properties. Therefore, the presence of contaminant gases is not detrimental for the target application.

1. Introduction

Radioactive waste packaging containing organic matter leads by radiolysis reactions to the generation of various gases, including hydrogen. For safety reasons, the amount of hydrogen must be limited to 4% vol., e.g. below the flammability limit. A solution to handle this problem might be to introduce a material in the package presenting high reactivity toward hydrogen gas in order to trap it and to ensure safe packaging, transportation and storage.

Intermetallic compounds (IMC) are known to react spontaneously with hydrogen to form metallic hydrides in wide ranges of temperature and pressure. They exhibit very high hydrogen volumetric densities and are ideal materials for the design of hydrogen getters. Such IMC able to store irreversibly hydrogen are known as Non Evaporable Getters (NEG) and are used nowadays for ultra-vacuum pumping [1], atmosphere purification [2] or tritium recovery in nuclear applications [3]. Among various IMC, the phases Zr_2Fe, ZrCo, ZrV_2 and Zr form very stable hydrides with plateau pressures around 10^{-6} MPa at ambient temperature and are used for commercial getter applications.

However, in the case of radioactive waste packaging, the thermodynamic conditions, the timescale and the nature and concentration of the gas in equilibrium with the IMC lead to very challenging conditions. The hydrogenation reaction proceeds through a dissociation step at the metal surface that can be strongly affected by the presence of inhibiting gas molecules. For example, carbon monoxide (CO) is known to be a fatal poison at ambient temperature for hydrogen absorption in IMC like $LaNi_5$ and Ti(Fe, Mn) [4]. In the present work, the hydrogen sorption properties of various Zr-based IMC have been investigated in the presence of 5% vol. of carbon monoxide.

2. Experimental

The compounds ZrCo and the Zr-rich Zr–Ti–V alloy were prepared by arc-melting of the pure elements (Zr, Co, V and Ti). Purities of raw materials were above 99% (Zirconium was slightly contaminated by 0.7% of Hafnium). The compounds have been annealed following the conditions reported in Table 1. The third compound of nominal composition Zr_2Fe was produced by the industrial company Cezus and was as-cast. X-ray diffraction experiments (XRD) were performed at room temperature on a Bruker AXS D8 θ–θ diffractometer using Cu-K_α radiation (λ = 1.5418 Å, Bragg–Brentano geometry, in beam rear graphite monochromator). The chemical composition of the phases was measured on bulk samples by electron probe microanalysis (EPMA) with a CAMECA SX100. The gas sorption properties were investigated using the Sievert method. Five hundred milligrams of samples are crushed and submitted to a primary vacuum (<1.10^{-2} mbar) before the first absorption. High purity gas (>99.999%) were used and the gas mixture (H_2 + 5 vol.%CO) were obtained by controlling the pressure and the temperature in gauged and calibrated tanks.

3. Results

3.1. Metallurgical characterization

Table 1 summarized the results from the XRD and the EPMA analysis for the three samples. The ZrCo compound contains two

---

[*] Corresponding author. Tel.: +33 1 49 78 12 10; fax: +33 1 49 78 12 03.
E-mail addresses: latroche@icmpe.cnrs.fr, latroche@glvt-cnrs.fr (M. Latroche).

0925-8388/$ – see front matter © 2010 Elsevier B.V. All rights reserved.
doi:10.1016/j.jallcom.2010.10.199

Table 1
Annealing conditions, chemical and structural analysis of the compounds.

Nominal composition	Annealing (time/temperature)	Chemical composition	Structural type	Phase amount (%wt.)
ZrCo	3 h/1000 °C	$Co_{50.0(4)}Zr_{49.6(4)}Hf_{0.35(4)}$	CsCl (*Pm-3m*)	94(1)
		$Co_{64(1)}Zr_{36(1)}$	$MgCu_2$ (*Fd-3m*)	6(1)
Zr–Ti–V alloy	7 days/1000 °C	$Zr_{85(1)}V_{8(1)}Ti_{6(1)}$	*hcp* ($P6_3/mmc$)	50(1)
		$Zr_{0.99(1)}[V_{1.93(1)}Ti_{0.08(1)}]$	$MgCu_2$ (*Fd-3m*)	50(1)
Zr_2Fe	as-cast	Zr_2Fe	Al_2Cu (*I4/mcm*)	60(1)
		Zr_3Fe	BRe_3 (*Cmcm*)	20(1)
		$ZrFe_2$	$MgCu_2$ (*Fd-3m*)	13(1)
		Zr	*hcp* ($P6_3/mmc$)	7(1)

phases. The main one corresponds to the expected ZrCo cubic phase (CsCl-type structure). Small precipitates of $ZrCo_2$ are also observed in accordance with the Zr–Co binary phase diagram [5]. This secondary phase can be explained by some Zr losses due to oxidation of this very reactive metal.

The Zr–Ti–V alloy also shows two phases with an extension of the *hcp* solid solution of zirconium and a ternary extension of the ZrV_2 intermetallic phase ($MgCu_2$-type structure), in accordance with the ternary phase diagram [6].

Finally, for the binary Zr–Fe system, beside the main intermetallic phase Zr_2Fe, three neighbouring phases of the phase diagram (Zr, Zr_3Fe and $ZrFe_2$) are also observed. Such result can be understood if one considers that the Zr_2Fe phase is only stable in a narrow temperature range between 780 °C and 951 °C [7]. Therefore, from the as-cast sample, it is not surprising to get a multiphase sample and an annealing treatment in the right temperature domain would be necessary to obtain a single-phase compound.

3.2. Gas sorption properties

The compound ZrCo was first submitted to 0.1 MPa of pure hydrogen (Fig. 1). At the first cycle, the absorption process starts after an activation period of 30 min. After 2 h, the reaction is completed and the compound absorbs 1.90 wt.% (2.87 H/f.u.). After a desorption step at 350 °C for 3 h under dynamic primary vacuum ($<10^{-2}$ mbar), the second absorption takes place in 12 s and leads to a capacity of 1.88 wt.% (2.85 H/f.u.), showing full reversibility of the sorption reaction and fast kinetic of the activated material. At the third cycle, the compound is submitted to a mixture of 94.9% vol. H_2 + 5.1% vol. CO (Fig. 4). The capacity reaches 0.49 wt.% (0.73 H/f.u.) after 85 h and the experiment was then interrupted. However, from Fig. 4 it can be seen that the absorption process was not slowing down at a function of time and one can expect larger capacity at longer time scale.

As for ZrCo, the compound Zr–Ti–V was first submitted to 0.1 MPa of pure hydrogen (Fig. 2). After an activation time of 30 min, the capacity reaches 2.33 wt.% (1.84 H/f.u.), in 45 min. The compound was desorbed at 350 °C during 3 h under dynamic vacuum and the second absorption occurs in 15 s but the capacity was strongly reduced (0.60 wt.% *i.e.* 0.47 H/f.u.). In the course of the first absorption, the two phases Zr- and ZrV_2-type absorb hydrogen. During the desorption step, only the ZrV_2 hydride can be decomposed according to the temperature range (350 °C), the ZrH_2 is too stable to be desorbed under these thermodynamic conditions [8]. The third absorption was realized after a desorption treatment at 500 °C for 2 h. The hydrogen uptake is as fast as for the second absorption and the capacity is slightly higher (0.90 wt.% *i.e.* 0.71 H/f.u.) in agreement with the higher applied desorption temperature. Nevertheless, part of the hydrogen remains trapped in the highly stable zirconium hydride phase. After a new desorption step for 2 h at 500 °C, the compound was submitted to a mixture of 94.5 vol.% H_2 + 5.51 vol.% CO (Fig. 4). After 45 h, the material has absorbed 0.31 wt.% (0.25 H/f.u.) and again, no slowing down of the reaction rate was observed.

For the Zr_2Fe compound, under 0.1 MPa of pure hydrogen (Fig. 3) the capacity at the first cycle reaches 1.88 wt.% (4.49 H/f.u.) but with relatively slow kinetics. After a desorption at 350 °C for 3 h under dynamic vacuum, the second and the third cycles are much faster (2 s) but the capacity decreases (respectively 1.18 wt.% (2.81 H/f.u.) and 0.84 wt.% (2 H/f.u.)). The absorption in the presence of carbon monoxide (Fig. 4) has been studied after desorption at 350 °C for 3 h under dynamic vacuum. In contact with a mixture of 94.85 vol.% H_2 + 5.15 vol.% of CO, the absorption rate is strongly reduced. The

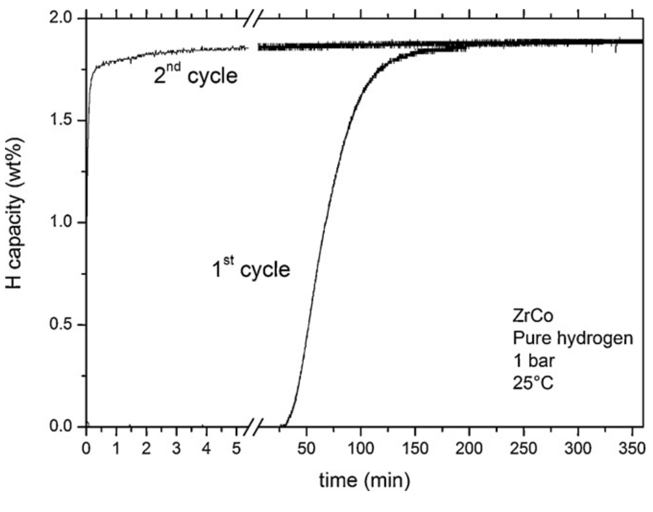

Fig. 1. Absorption kinetics of the ZrCo compound. The first cycle is characterized by an activation time followed by the absorption step.

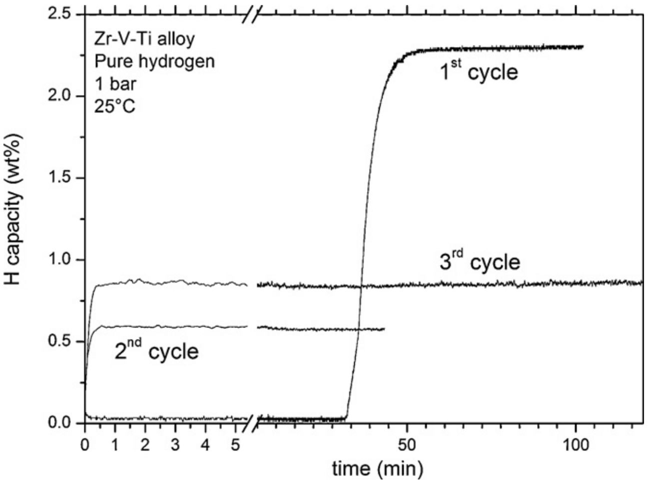

Fig. 2. Hydrogen capacity as a function of time for the Zr–Ti–V alloy. The first cycle is characterized by an activation time followed by the absorption step. Capacities of the 2nd and 3rd cycles are less that of the first one.

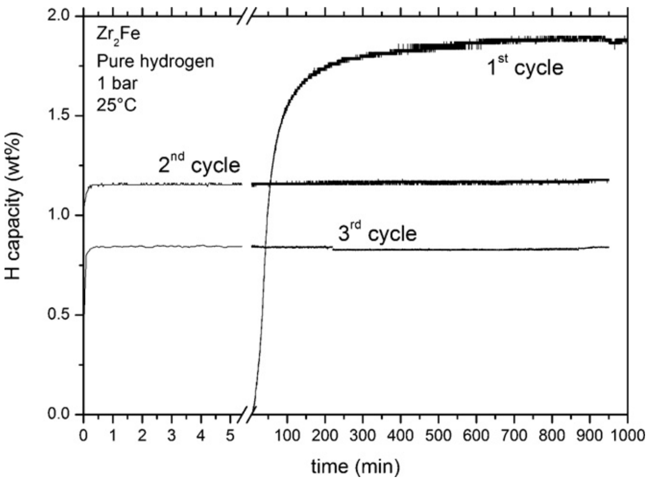

Fig. 3. Hydrogen capacity as a function of time for the Zr_2Fe compound. The first cycle is characterized by a short activation time followed by the absorption step. Capacities of the 2nd and 3rd cycles are less that the first one.

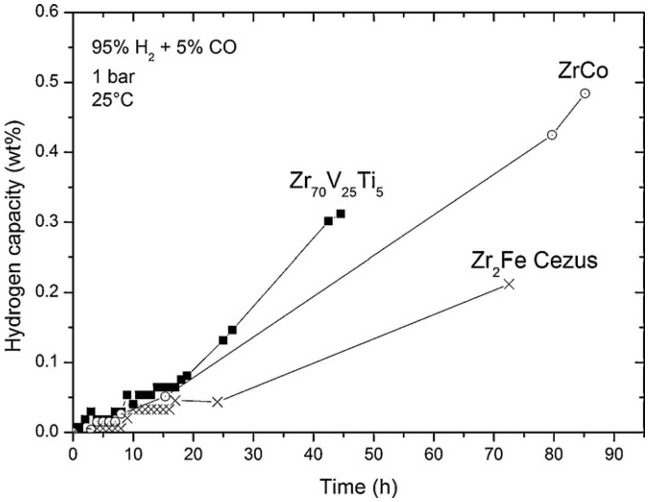

Fig. 4. Hydrogen sorption capacities as a function of time for the three Zr-based compounds ZrCo, Zr_2Fe and Zr–Ti–V alloy (after activation) in presence of 5 vol.% of carbon monoxide.

capacity is 0.21 wt.% (0.50 H/f.u.), after 72 h which corresponds to 25% of the capacity measured at the third cycle. As for the two previous samples, the reaction was interrupted though the absorption process was still running showing that the equilibrium was not yet reached.

4. Discussion

With pure hydrogen and at the first cycle, the absorption properties for the three studied compounds are in agreement with the expected values reported in the literature. However, different activation times are observed depending on the alloy composition. For the second and the third cycles, capacities are lower (except for ZrCo) and this is attributed to the formation of highly stable hydrides like ZrH_2 for Zr–Ti–V alloy or Zr_3FeH_2 for Zr_2Fe that cannot be desorbed under the applied desorption treatment.

Table 2
Absorption rate for H_2 and H_2 + CO for the activated compounds.

Compound	Pure H_2 (wt.%)/s	H_2 + CO 5% vol. (wt.%)/day
ZrCo	0.14	0.10
Zr–Ti–V alloy	0.05	0.12
Zr_2Fe	0.38	0.04

In the presence of 5 vol.% of carbon monoxide, our data show that hydrogenation process still occurs for the three Zr-based compounds ZrCo, Zr–Ti–V alloy and Zr_2Fe. However, the presence of CO contaminant significantly slows down the absorption rates (Table 2) as compared to the values reported for pure hydrogen. Nevertheless, the absorption rates are significant enough for ZrCo and Zr–Ti–V alloy (about 0.1% wt. per day) and the curves reported in Fig. 4 do not exhibit any deceleration so higher capacities are expected at longer timescale. Such hydrogenation properties may be convenient to design hydrogen getter apparatus to be used in conditions where hydrogen is generated at slow rates. Among the three compounds, Zr–Ti–V alloy shows the fastest rate and the highest capacity.

Contrary to other intermetallic like $LaNi_5$ and Ti(Fe, Mn), the presence of carbon dioxide is not detrimental for hydrogen storage in the materials tested here. The decrease of kinetic is explained by the adsorption of CO molecules at the surface of the materials. Sandrock et al. [4] observed that CO molecules block the active sites constituted by surface atoms (Ni and Ti) creating carbonyl group or partial oxidation and carburizing. In the case of zirconium based compounds, the physico-chemistry of CO adsorption might be different. Moreover, Ti(Fe, Mn) and $LaNi_5$ compounds have plateau pressures closed to 0.1 MPa at room temperature. In the case of Zr-alloys, the absorption pressures are much lower (10^{-6} to 10^{-7} MPa at ambient temperature) leading to a larger driving force for hydrogenation. Finally, it is worth to note that in the case of ZrCo, the compound is single phase and its absorption properties are intrinsic. On the contrary, for the Zr–Ti–V alloy and the Zr_2Fe compound, several phases coexist and the gas sorption properties of each phase should be considered in details regarding carbon monoxide poisoning and potential cooperative effects between coexisting phases.

5. Conclusion

Three Zr-based compounds ZrCo, Zr-rich Zr–Ti–V alloy, and Zr_2Fe have been studied as hydrogen sorption materials in the presence of carbon monoxide. It is shown that though the sorption reaction is strongly slowed down by comparison to pure hydrogen, CO at low concentration is not a fatal poison for the studied compounds and absorption may occur at a satisfactory rate (0.1 wt.%/day). Such sorption rate could be sufficient to control hydrogen pressure in environments for which H_2 production occurs very slowly.

References

[1] C. Benvenuti, P. Chiggiato, P.C. Pinto, A.E. Santana, T. Hedley, A. Mongelluzzo, V. Ruzinov, I. Wevers, Vacuum 60 (1–2) (2001) 57–65.
[2] S. Fukada, K. Tokunaga, M. Nishikawa, Fusion Engineering and Design 36 (1997) 471–478.
[3] T. Nagasaki, S. Konishi, H. Katsuta, Y. Naruse, Fusion Technology 9 (1986) 506–509.
[4] G.D. Sandrock, P.D. Goodell, Journal of the Less Common Metals 104 (1) (1984) 159–173.
[5] T.B. Massalski, Binary Alloy Phase Diagrams, second ed., ASM International, Materials Park, OH, USA, 1990.
[6] P. Villars, A. Prince, H. Okamoto, Handbook of Ternary Alloy Phase Diagrams, ASM International, Material Park, OH, USA, 1997.
[7] F. Stein, G. Sauthoff, M. Palm, Journal of Phase Equilibria 23 (6) (2002) 480–494.
[8] E. Zuzek, J.P. Abriata, A. San-Martin, F.D. Manchester, H–Zr (Hydrogen–Zirconium) Phase Diagrams of Binary Hydrogen Alloys, ASM International, Materials Park, OH, USA, 2000, pp. 309–322.